Article citation info:
LIANG H, MI J, BAI L, CHENG Y. Imprecise sensitivity analysis of system reliability based on the Bayesian network and probability box. Eksploatacja i Niezawodnosc – Maintenance and Reliability 2020; 22 (3): 508–519, http://dx.doi.org/10.17531/ein.2020.3.14.

He LIANG
Jinhua MI
Libing BAI
Yuhua CHENG

IMPRECISE SENSITIVITY ANALYSIS OF SYSTEM RELIABILITY BASED ON THE BAYESIAN NETWORK AND PROBABILITY BOX

NIEDOKŁADNA ANALIZA CZUŁOŚCIOWA NIEZAWODNOŚCI SYSTEMU W OPARCIU O SIEĆ BAYESOWSKĄ I POLE PRAWDOPODOBIEŃSTWA (P-BOX)

Sensitivity analysis measures how changes in system inputs affect outputs. Previously, a large amount of sensitivity analysis research was relevant to the precise probability that is regarded as an ideal condition of engineering. Due to insufficient test samples and the low accuracy of test data, system reliability with hybrid uncertainty is difficult to be described as a precise value. As a profusion of highly integrated electromechanical equipment is applied in modern life, it is impossible to apply sufficient resources to eliminate the stochastic property of every component, which necessitates the identification of highly sensitive components to efficiently reduce imprecision. Hence, based on the theory of imprecise probability, imprecise sensitivity analysis has become a popular research topic in the last decade. In this paper, a method for uncertain system reliability and imprecise sensitivity analysis is proposed based on a Bayesian network, a probability box and the pinching method. The feasibility and accuracy of the combined method are fully verified through the evaluation and analysis of a numerical example and a case study of an electromechanical system, and the highly sensitive components that heavily influence the imprecision of system outputs are accurately identified.

Keywords: *bayesian network; probability box; sensitivity analysis; reliability analysis.*

Celem analizy czułościowej jest badanie w jakim stopniu zmiany danych wejściowych systemu wpływają na dane wyjściowe. Dotychczasowe badania z wykorzystaniem analizy czułościowej były związane z dokładnym prawdopodobieństwem postrzeganym w inżynierii jako warunek idealny. Przy niewystarczającej wielkości badanej próby i niskiej dokładności danych testowych, niezawodność systemu o hybrydowej niepewności trudno opisać w sposób dokładny. Biorąc pod uwagę fakt, że we współczesnym świecie wykorzystuje się duże ilości wysoce zintegrowanych urządzeń elektromechanicznych, niemożliwa jest alokacja wystarczających zasobów w celu wyeliminowania właściwości stochastycznych każdego elementu. Oznacza to, że aby zredukować niedokładność, konieczna jest identyfikacja komponentów o wysokiej czułości. Dlatego też popularnym przedmiotem badań ostatniej dekady stała się niedokładna analiza czułości, bazująca na teorii niedokładnego prawdopodobieństwa. W artykule zaproponowano metodę analizy niezawodności niepewnego systemu jak również niedokładnej analizy czułościowej w oparciu o sieć bayesowską, pole prawdopodobieństwa i metodę pinch point. Możliwość wykorzystania i dokładność metody zostały w pełni potwierdzone na podstawie przykładu liczbowego jak również studium przypadku systemu elektromechanicznego; proponowana metoda pozwoliła na poprawne określenie wysoce czułych elementów systemu, które w dużym stopniu wpływają na niedokładność danych wyjściowych układu.

Słowa kluczowe: *sieć bayesowska; pole prawdopodobieństwa; analiza czułości; analiza niezawodności.*

1. Introduction

With the improvement of industrial techniques and requirements for productivity, plenty of high-integrity and complex-structured electromechanical systems (EMSs) have been widely employed and utilized. The performance of the equipment can be further enhanced with a higher integration, which necessitates a better understanding of the failure degradation law of key components. For the design of a highly integrated system, reliability theory has attracted considerable researches in recent years to study the failure relationship among systems and components with the lifetime of products as the main research object. Specifically, many strategies have been proposed for the sake of reliability model establishment, such as block diagrams [1], Markov analysis (MA) [2], simplified equations [3] and fault trees (FTs) [4]. An FT is a powerful tool for reliability modeling that uses binary decision diagrams (BDDs). As an extension of an FT, a Bayesian network (BN) describes the relationship of failure events with a directed acyclic graph (DAG) as well as conditional probability tables (CPTs), as proposed by Pearl [5], achieving significant development in system reliability and safety analyses. In addition, Cai et al. [6] evaluated the reliability of a blowout preventer control system with a BN. A BN model was also established for wind turbines by Su et al. [7] to achieve a reliability analysis considering environmental factors and uncertainty. Mi et al. [8] presented a methodology to quantify the importance of common cause failures in the context of a BN and probability bounds analysis.

The uncertainty of the system is very important for the accuracy of the reliability estimation since it is difficult to attain a comprehensive knowledge of system failure. Specifically, in simulation and experimental processes, according to Ref. [9], uncertainties can be divided into three sources:

1) Uncertainties in parameterization.
2) Uncertainties in modeling.
3) Uncertainties in experiments.

However, to reduce the effects of uncertainty, it is more advantageous to take the intuitive uncertainty quantification metrics and the adjustment of the reliability analysis into prior consideration.

Uncertainty is currently divided into two types: epistemic (reducible) uncertainty and aleatory (irreducible) uncertainty [10, 11]. Aleatory uncertainty, determined by the random properties of a system, cannot be reduced, whereas the probability distribution can be derived easily by classic probability theory. However, epistemic uncertainty caused by the lack of knowledge of system mechanisms and samples cannot be eliminated by classic probability methods. Although the effects of epistemic uncertainty can be diminished through mass testing data and a deep understanding of system mechanisms, experts have not reached a consensus on dealing with epistemic uncertainty at present except for taking its quantification under initial consideration. The theory of evidence was first proposed by Dempster and then further promoted by Shafter, so it is called D-S evidence theory [12]. Basically, it can be interpreted as a generalization of Bayesian probability, assigning a number between 0 and 1 to the degree of belief supporting a certain proposal [13]. The details of the definitions refer to references [13–15]. Miscuri et al. [13] utilized an evidence network, which is the combination of the BN and evidence theory, and critical networks for security vulnerability assessment. In addition to evidence theory, probability bounds theory (PBA), also known as the probability box (p-box), is another popular uncertainty quantification metric. Based on precise probability theory, the p-box is divided into parametric and nonparametric types. The parametric p-box assumes that the probability distributions of the variables are known, and the possible cumulative distribution functions (CDFs) of the variable are in the same distribution. However, for the nonparametric p-box, the CDFs can be any CDF between the lower and upper probability bounds. Mi et al. [16] constructed a p-box to characterize the uncertainty of a multistate system with CCF. Feng et al. [17] evaluated sensitivity by utilizing the p-box as the quantification metric and a survival signature as the reliability modeling method. Meanwhile, Schöbi et al. [18] proposed interval-valued Sobol indices as an extension of classic definition by modeling the uncertain input parameters through parametric p-boxes. In short, the p-box is suitable for illustrating the epistemic uncertainty caused by insufficient samples, while it is more beneficial to consider evidence theory for the uncertainty caused by low data accuracy [19]. As Ref. [20] concludes, for any event $U \in F$, the upper and lower probability bounds respectively correspond to the belief function $Bel(U)$ and plausibility function $Pl(U)$, in which we can find the mutual conversion of evidence theory and p-box in the mathematical form.

Sensitivity analysis (SA) quantifies the influence of input uncertainty variation on the system output uncertainty. The purpose is to determine the main source of the system uncertainties. SA provides a basis for uncertainty reduction and can improve the robustness of the model prediction. Traditionally, SA methods for precise probability distribution have been developed rapidly, and various approaches have been proposed, such as regional sensitivity analysis [21] and matrix-based metrics [22].

However, there are still few publications for imprecise sensitivity analysis (ISA) [18]. Sankararaman & Mahadevan [23] and Krzykacz-Hausmann [24] described a global SA in the presence of Bayesian hierarchical models. Ref. [25] introduced Sobol indices for ISA. In addition, Helton et al. [26], on the basis of evidence theory, discussed the variance-based algorithm. The pinching method, proposed by Ferson [27], compares the variation in output uncertainty when part of the input variables has eliminated the uncertainty as a precise value, interval or probability distribution.

In response to the necessity of ISA studies of uncertain system reliability, this paper proposes a method to establish a reliability model with a BN, using the pinching method [27] to complete sensitivity analysis with the imprecision characterized by the p-box. Then, the high-sensitivity components and subsystems can be identified by ranking the indices. This approach is introduced as a new solution that implements the Bayesian network and pinching method for reliability and sensitivity analysis. A numerical example and an EMS case are detailed and analyzed by the proposed ISA approach to verify its feasibility. Hence, this article is organized as follows. Section 2 introduces the reliability, uncertainty, and sensitivity analysis theories involved in the following cases. Using an example of an uncertain system, details of the reliability modeling and sensitivity analysis are described in Section 3. In Section 4, the proposed method is applied to an EMS. Conclusions are provided in Section 5.

2. Preliminaries

2.1. Bayesian network

A BN consists of a DAG and CPTs, representing the direct dependency probability relationships among the variables [28]. Fig. 1 shows a simple BN, where the texts in the circles refer to certain failure events, and the directed arrows indicate the relationship of events. In the graph, nodes with only outputs are named root nodes, whereas leaf nodes have only inputs. Therefore, the clear and brief form to illustrate the propagation of failures is the advantage of a DAG. For constructing CPTs in the reliability and safety field, when the logic relation of parent nodes is AND, it means that the child event could be true only if parent events are true. Moreover, if the logic relation is OR, the child event will be true as long as one parent event is true. Notably, to optimize the calculation, CPTs should follow some format specifications. In this paper, "F" refers to the fail state of the component and "T" refers to the normal state. As a proposition regarding whether the given component state is true in the CPT table, "1" means true, and "0" means false. It is assumed that X_1 is in series with X_2 and that X_3 is in parallel with Y. As shown in Table 1 and Table 2, the tables that describe the marginal probability distribution of Y and T are CPTs, and the two tables depict the logic relation of AND and OR, respectively.

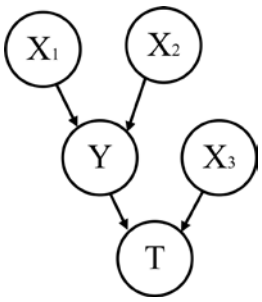

Fig. 1. A simple BN

Table 1. CPT of intermediate node Y

X_1	X_2	Y	
		F	T
F	F	1	0
F	T	0	1
T	F	0	1
T	T	0	1

The reasoning of the BN consists of forward and backward inference, also termed as predictive and diagnostic analysis, respectively. The former infers the marginal probability of any node in the condition of a given parent node's prior marginal probability mass function (PMF) and conditional PMFs of other child nodes in the network.

Table 2. CPT of leaf node T

X_1	X_2	T	
		F	T
F	F	1	0
F	T	1	0
T	F	1	0
T	T	0	1

Assuming that a set of random variables $\{X_1,...,X_n\}$ is composed of the system failure events corresponding to each node in a BN, the joint distribution can be calculated by the following formula:

$$P\{X_1,...,X_n\}=\prod_{i=1}^{n}P(X_i|\pi_i) \tag{1}$$

where π_i is the parent node of X_i. For the BN shown in Fig. 1, the joint probability distribution is given by Eq. (2):

$$P\{T,Y,X_1,X_2,X_3\}=P(T|X_3,Y)P(Y|X_1,X_2)P(X_3)P(X_2)P(X_1) \tag{2}$$

Using Eq. (1), the marginal probability distribution of X_i can be presented as:

$$P\{X_i\}=\sum_{except\ X_i}P\{X_1,...,X_n\} \tag{3}$$

With R defined as the reliability of the system, the reliability of the system shown in Fig. 1 can be presented as:

$$R=1-\sum_{except\ T}P\{X_1,X_2,X_3,\mathrm{Y},\mathrm{T}\} \tag{4}$$

2.2. Probability box

For a system with aleatory uncertainty, precise probability distributions can be used to quantify the degree of uncertainty, such as exponential, Weibull, and lognormal distributions. Consequently, classic probability theory exhibits favorable performance for quantitative issues of aleatory uncertainty. However, due to the incomplete knowledge of the system mechanism and the sample data, epistemic uncertainty always exists in the system. Furthermore, the classic probability method is not the appropriate evaluation approach because of the probability parameters defined as the intervals. To precisely measure the system uncertainty, the p-box is a solution providing a clear view of the epistemic uncertainty of a random variable and has been widely applied to quantify and represent the uncertainty in risk analysis [29] [10]. A nonnegative random variable X describes the lifetime of a component. $F_L(t)$ and $F^U(t)$ are CDFs of variable X on real number R, and $F(t)=P\{X\le t\}$. Suppose F is a set of nondecreasing functions that map R into [0,1], where $F_L(t)$ and $F^U(t)$ are the lower and upper bounds of F. Then, a p-box is defined by a probability family that matches the constraints $F_L(t)\le F(t)\le F^U(t)$ and $F(t)\in$F [10]. For reliability $R(t)=1-F(t)$, the p-box $\Re$ reflects the survival probability and is defined as:

$$\Re=\left\{R(t),\forall t\in R\middle|R_L(t)\le R(t)\le R^U(t)\right\} \tag{5}$$

For example, suppose the random variable X_{wb} follows a Weibull distribution, the shape and scale parameters are set as $\beta=3$ and $\eta=[10,40]$, respectively, and the parameters for the lognormal distribution X_{Logn} are $\sigma=0.4$ and $\mu=[6,8]$. As shown in Fig. 2, the p-boxes describe the reliability bounds by $R_L(X_{wb})$, $R^U(X_{wb})$, $R_L(X_{Logn})$ and $R^U(X_{Logn})$, and the uncertainty can be quantified as the regions of S_{wb} and S_{Logn}. The area of epistemic uncertainty space enclosed by the upper and lower bounds can be converted from graphs to numerical form via Eq. (6):

$$S_s=\int_0^{+\infty}(1-F_L(t))dt-\int_0^{+\infty}(1-F^U(t))dt=\int_0^{+\infty}R^U(t)dt-\int_0^{+\infty}R_L(t)dt=ET^U-ET_L. \tag{6}$$

where ET^U and ET_L represent the maximum and minimum mean lifetimes of the system, respectively. Eq. (6) quantifies the variation of system reliability with epistemic uncertainty, providing an index for uncertainty reduction. Moreover, the index is calculated for SA in the next subsection.

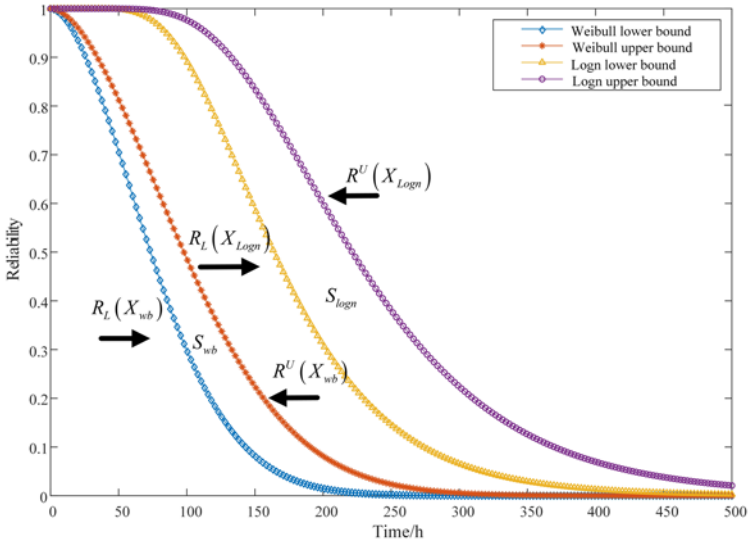

Fig. 2. P-boxes of Weibull and lognormal distributions

2.3. Sensitivity analysis of reliability

It has been shown that increasing the quantity and improving the accuracy of samples can reduce the epistemic uncertainty, but this is difficult to achieve for every component in a complex system. System reliability SA [30] [26] identifies the high-sensitivity components and optimizes their uncertainty properties to enhance equipment performance and save resources. Therefore, a variety of SA metrics have been developed for better performance to solve practical engineering issues.

In engineering practice, since the precise distribution is always unknown, an interval value is used for uncertainty prediction, and traditional SA methods are invalid due to the imprecise form of input variables. Ferson [27] proposed the p-box to characterize this uncertainty, which merges interval analysis and classic probability theory and treats aleatory and epistemic uncertainty separately on the basis of maintaining their features. The p-box permits a comprehensive uncertainty analysis, and this fact obviates some of the complexity that afflicts traditional Monte Carlo approaches to sensitivity analysis based on similar ideas. Based on the uncertainty definition by the p-box, the sensitivity index S_e can be computed by Eq. (7):

$$S_e=1-\frac{un(\mathrm{A})}{un(B)} \tag{7}$$

where B is the initial value of the epistemic uncertainty and A is the uncertainty index when the input epistemic uncertainty is reduced. Moreover, $un()$ represents the uncertainty quantification method, which can be described by the p-box graph and calculated through the size of the uncertainty space enclosed by the probability bound; the details can be seen in Section 2.2.

To identify highly sensitive components, the pinching method should be initially used to reduce the uncertainty of each component, followed by evaluating and ranking the sensitivity indexes obtained by Eq. (7). It should be noted that, unlike the variance-based index, the uncertainty reduction will not add up to 100% after all the input variables eliminate the uncertainty.

There are multiple possibilities to pinch uncertainty. Different pinching strategies provide diverse sensitivity values but will not affect the ranking of the values. The three different strategies are listed as follows [27]:

(i) replace an input with a point value,
(ii) replace an input with a precise distribution function, or
(iii) replace an input with a zero-variance interval.

Considering that aleatory uncertainty is easy to model by classic probability theory but hard to eliminate, this work selects strategy (ii) to pinch the uncertainty, which focuses on the characterization of aleatory uncertainty and the elimination of epistemic uncertainty. Due to the unknown target parameter value after pinching uncertainty, different target values used in the SA cause changes in index values, which is termed the deviation. To reduce the effect of deviation, a new sensitivity index that takes the means of all sensitivity index values is proposed and is shown as Eq. (8):

$$S_{mean}=\frac{1}{l_s}\sum_{i=0}^{l_s}1-\frac{un(\mathrm{A}_i)}{un(B)} \tag{8}$$

where l_s is the sampling value of the random variable parameter.

3. Reliability sensitivity analysis for an uncertain system

3.1. Analysis process

In this section, a comprehensive work for reliability sensitivity analysis is presented, and there are 3 steps for the ISA of system reliability, as shown in Fig. 3.

i Preprocessing: The aim of this step is to determine the distribution of pinched variables and construct the input vectors. Furthermore, based on the failure mechanism of the system, the BN model needs to be prepared for forward inference to evaluate system reliability.

ii Uncertain system reliability analysis: Via the inference of the BN, the probability distribution families of system reliability in the case of pinched input variables and initial inputs are obtained. Next, a p-box is employed to quantify the uncertainty and visualize it. The uncertainty quantification index is defined as the size of the region enclosed by probability bounds.

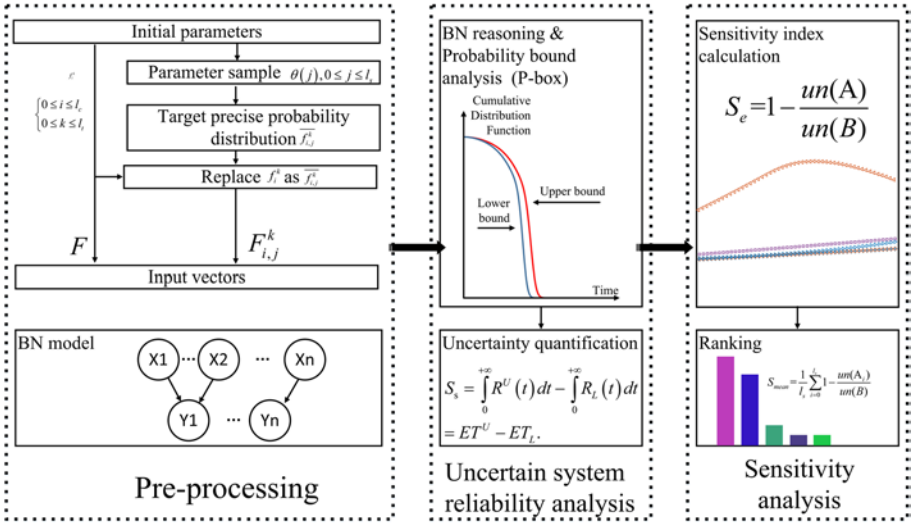

Fig. 3. The analysis process of this work

iii Sensitivity analysis: Because of the deviation of the sensitivity, computation of the mean of sensitivity values as the ultimate index of sensitivity assessment is applied to reduce the effect of deviation, which briefly indicates the highly sensitive components in the system.

The detailed analysis process will be described in the following sections.

3.2. Preprocessing

3.2.1. Input vectors

Assume that a system consists of l_c components in l_t different types, where the index of a component is defined as i, k refers to the type index, and that they match the constraints $k\in\{1,2,\ldots,l_t\}$ and $i\in\{1,2,\ldots,l_c\}$. For example, f_i^k expresses the failure probability of component i with type k. The input vector in the condition that no variable is pinched is written as the initial vector $F=\left[f_1^1,\ldots,f_i^k,\ldots,f_{l_c}^{l_t}\right]$. Then, as Section 2.3 describes, when f_i^k is pinched, the epistemic uncertainty of the i-th component with type k. is hypothetically eliminated. Hence, suppose $\overline{f_i^k}$ is the distribution f_i^k after pinching. Moreover, f_i^k will be replaced by $\overline{f_i^k}$ in the initial input vector. The input vector F will be renewed and written as F_i^k, where $F_i^k=\left[f_1^1,\ldots,\overline{f_i^k},\ldots,f_{l_c}^{l_t}\right]$. For instance, in the case of f_5^2 being pinched, the F_5^2 matches the equation $F_5^2=\left[f_1^1,\ldots,\overline{f_5^2},\ldots,f_{13}^5\right]$. Because the target of pinching is just a hypothesis, diverse target parameters lead to different input vectors, obviously affecting the ISA results, which is called deviation. Therefore, f_i^k is sampled with sample value l_s for comprehensive analysis results and defined by target parameter $\theta(j)(0<j\le l_s)$ as $\overline{f_{i,j}^k}$. Similarly, f_i^k is replaced by $\overline{f_{i,j}^k}$ for an input vector, where $F_{i,j}^k=\left[f_{1,j}^1,\ldots,\overline{f}_{i,j}^k,\ldots,f_{l_c,j}^{l_t}\right]$. Similar to the above example, when $l_s=10000$ and the target parameter is $\theta(400)$, the input vector is written as $F_{5,400}^2=\left[f_1^1,\ldots,\overline{f_{5,400}^2},\ldots,f_{13}^5\right]$.

3.2.2 BN modeling

According to Section 3.2.1, the input vector $F_{i,j}^k$ when the probability distribution of component i is pinched, uncertainty is obtained.

Subsequently, the following matrix D can be used to illustrate the relationships of each DAG node shown as Eq. (9):

$$D=\begin{bmatrix} d_{1,dm} & \cdots & d_{1,dm} \\ \vdots & \ddots & \vdots \\ d_{1,dm} & \cdots & d_{22,dm} \end{bmatrix} \tag{9}$$

where $d_{a,}$b=1 means the arrow in the DAG moves from node a to node b. When there is no connection between a and b, $d_{a,c}$=0. After matrix D is obtained from the BN model, referring to Table 1 and Table 2, the CPTs of the child nodes in the DAG can be listed in the form of a column vector to participate in the forward inference.

3.3 Uncertainty system reliability analysis

Combining Eq. (3) with Eq. (1), the marginal probability distribution of child nodes can be written as:

$$P\{\mathrm{n}\}=\mathrm{CPT_n}\prod_{i=p}P(\pi_i) \tag{10}$$

where n is the child node, π_i is a parent node, and p is the number of parent nodes. Therefore, $P\{\mathrm{n}\}$ represents the marginal probability of the failure events of child nodes. Similarly, $P\{\pi_i\}$ are the marginal probabilities for parent nodes. This formula accomplishes BN forward inference and deduces the system reliability.

Eq. (10) can be used to compute marginal probability when input variables are precise probability distributions. However, uncertainty exists in the parameters of $F_{i,j}^{k}$, and it is necessary to sample the parameters. Assume the sample value for BN inference is l_{bn}. Consequently, the input vector after sampling is $F_{i,j,m}^{k}=\left[f_{1,j,m}^{1},\ldots,\overline{f}_{i,j,m}^{k},\ldots,f_{l_c,j,m}^{l_t}\right]$. $P_{i,j,m}^{k}\{n\}$ can be written as:

$$P_{i,j,m}^{k}\{n\}=CPT_n\times\prod_{i=n_k}\left(F_{i,j,m}^{k}\times D_n\right) \tag{11}$$

where $P_{i,j,m}^{k}\{n\}$ is the probability of the event represented by the child node n. $F_{i,j,m}^{k}$ should add zeros to expand the size and be assigned during the iterations. The reliability can be written as:

$$R_{i,j,m}^{k}=1-P_{i,j,m}^{k}\{A\} \tag{12}$$

3.4. Sensitivity analysis

The pinching method is applied to analyze the sensitivity by eliminating the epistemic uncertainty of a variable and computing the change in the output uncertainty. To overcome the deviation issue of determining different target parameters *θ(j)*, the size of the area that is enclosed by the upper and lower bounds of the p-box should be calculated as the uncertainty quantification index. Then, based on the computed uncertainty index, the sensitivity index can be obtained by definition in Eq. (8).

3.5. Numerical example

In this section, a complex nonrepairable system from Ref. [31], composed of thirteen components with five different types, is described to demonstrate the effectiveness of the proposed method. Note that numbers in the solid line and the lower right corner denote the type of the component and the serial number, respectively, while Roman numerals and English letters represent subsystems. Table 3 gives the type of probability distributions and parameter ranges of each component, where η and β are the scale parameter with the hour unit and the nondimensional shape parameter of the Weibull distribution, respectively. Meanwhile, the λ of the exponential distribution represents its mean value with the same unit as η.

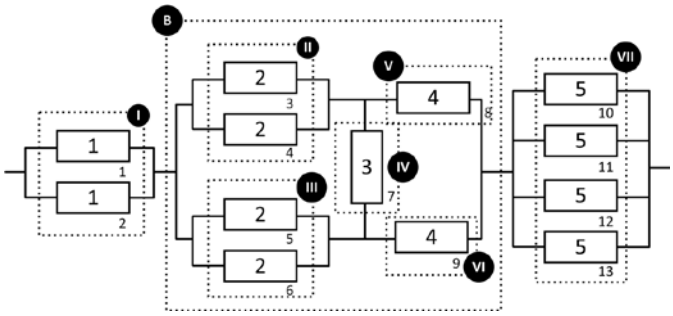

Fig. 4. A block diagram of a nonrepairable system [31]

Table 3. Probability distributions with epistemic and aleatory uncertainty of 5 types of components

Type	Distribution	Parameter (with epistemic uncertainty)
1	Weibull	$\eta_1=[1.68,1.86],\beta_1=2.08$
2	Exponential	$\lambda_2=[1.07,1.33]$
3	Weibull	$\eta_3=[2.12,2.51],\beta_3=1.38$
4	Weibull	$\eta_4=[2.99,3.41],\beta_4=2.51$
5	Exponential	$\lambda_5=[2.01,2.28]$

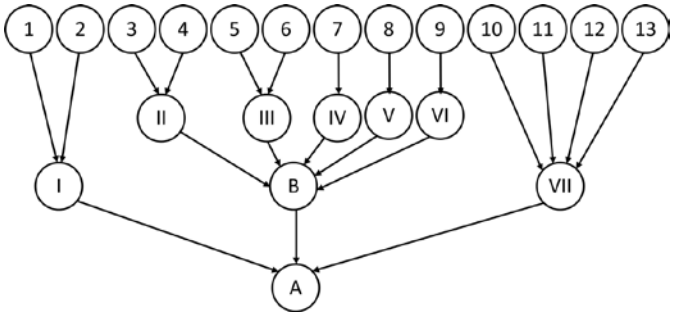

Fig. 5. BN of the system

Based on the definitions described above, the DAG shown in Fig. 5 could be transformed into the following matrix by Eq. (13) and Eq. (14).

$$D=\begin{bmatrix} d_{1,1} & \cdots & d_{1,22} \\ \vdots & \ddots & \vdots \\ d_{1,22} & \cdots & d_{22,22} \end{bmatrix} \tag{13}$$

where

$$\begin{cases} d_{1,14} = d_{2,14} = 1 \\ d_{3,15} = d_{4,15} = 1 \\ d_{5,16} = d_{6,16} = 1 \\ d_{7,17} = 1 \\ d_{8,18} = d_{9,19} = 1 \\ d_{10,20} = d_{11,20} = d_{12,20} = d_{13,20} = 1 \\ d_{15,21} = d_{16,21} = d_{17,21} = d_{18,21} = 1 \\ d_{14,22} = d_{21,22} = d_{20,22} = 1 \\ \text{else} = 0 \end{cases} \tag{14}$$

Furthermore, the CPT of each intermediate node in Fig. 5 can be established according to Section 3.3. For example, Table 4 shows the CPT of leaf node A based on the standards and specifications detailed in Section 2.1.

Note that it is more advantageous to express CPTs in a matrix form to simplify calculations. However, since subsystems II, III, IV, V, VI, and VII are not logical AND gates or OR gates, the CPT of node B must be listed separately. As shown in Table 5, CPT_B is a column vector with a length of $2^6 \times 1$.

Table 4. CPT of subsystem A

1	2	A	
		F	T
F	F	1	0
F	T	1	0
T	F	1	0
T	T	0	1

Table 5. CPT of subsystem B

II	III	IV	V	VI	B	
					F	T
F	F	F	F	F	1	0
T	F	F	F	F	1	0
F	T	F	F	F	1	0
...	...	...	...	...	...	...
T	F	T	T	T	0	1
F	T	T	T	T	0	1
T	T	T	T	T	0	1

Fig. 6 depicts the reliability p-box of each type component under different input vectors in the system according to the method described in Section 3.3. The impact of the components with the same connection methods, as well as failure probability distributions, can be considered equivalent. Therefore, simplification should be taken into prior consideration in reliability modeling. From the results shown in Fig. 7, we find that the probability bounds of the system reliability obtained by the uncertainty pinching of the same type of components completely overlap. Thus, we can conclude that for sensitivity analysis, the components with the same type and connection are of equivalence. Hence, only one component for each type needs to be selected to perform SA.

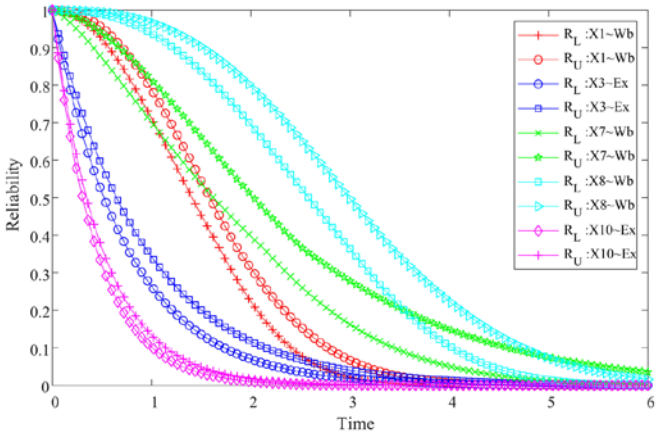

Fig. 6. Reliability p-box of different component types (X1, X3, X7, X8 and X10 refer to component types 1-5, respectively).

Fig. 8 depicts the p-box of the system reliability when the uncertainty of the random variables X1, X3, X7, X9 and X10 are pinched. Compared with the initial bounds, the bounds after pinching are slightly contracted. However, there may exist crossover and overlapping parts for the curves shown in Fig. 8, and it is difficult to compare the uncertainty space of p-boxes directly. Hence, it is more beneficial to define an index to quantify the uncertainty space of the system to further quantify the sensitivity. Therefore, measuring the size of the upper and lower areas is an appropriate method for uncertainty quantification. The ISA approach was described in Section 3.4.

With different values of the target parameter $\theta(j)$, the sensitivity of the component will change differently, which is denoted as the deviation. Fig. 9 shows the sensitivity deviation of components with different types. It is clear that the sensitivity of the type 5 components is significantly higher than others, which means that the uncertainty reduction in type 5 components will cause the greatest influence on the uncertainty of system reliability. However, the sensitivity of type 3 and type 4 components are much lower than other types, and it is hard to identify the type with the lowest sensitivity due to the sensitivity variation. According to Section 2.3, the influence of deviation can be reduced by the proposed method by calculating the mean value with Eq. (8). Fig. 10 shows a bar plot of the sensitivity of the components, and it can be clearly observed that the type 5 components are the most sensitive. Conversely, type 3 component X7 is the most insensitive component.

4. Case study

4.1. Description of the case

In Section 3, a comprehensive method is proposed for analyzing the reliability and sensitivity of the system, and a numerical example is introduced to detail the steps of the method. However, in a practical engineering system, the degradation of the components directly causes the working efficiency reduction, and the lack of sample data will also lead to the existence of uncertainty and nonlinear characteristics in a system. In this section, the proposed method is used to analyze the reliability and sensitivity of the electromechanical system in Ref. [10]. Fig. 11 shows the schematic of this electromechanical system, which is composed of a control system, a power supply system, a powertrain system, and a hydraulic system. More specifically, the control system includes two control modules connected in parallel to perform the start-stop control of the main valve and control execu-

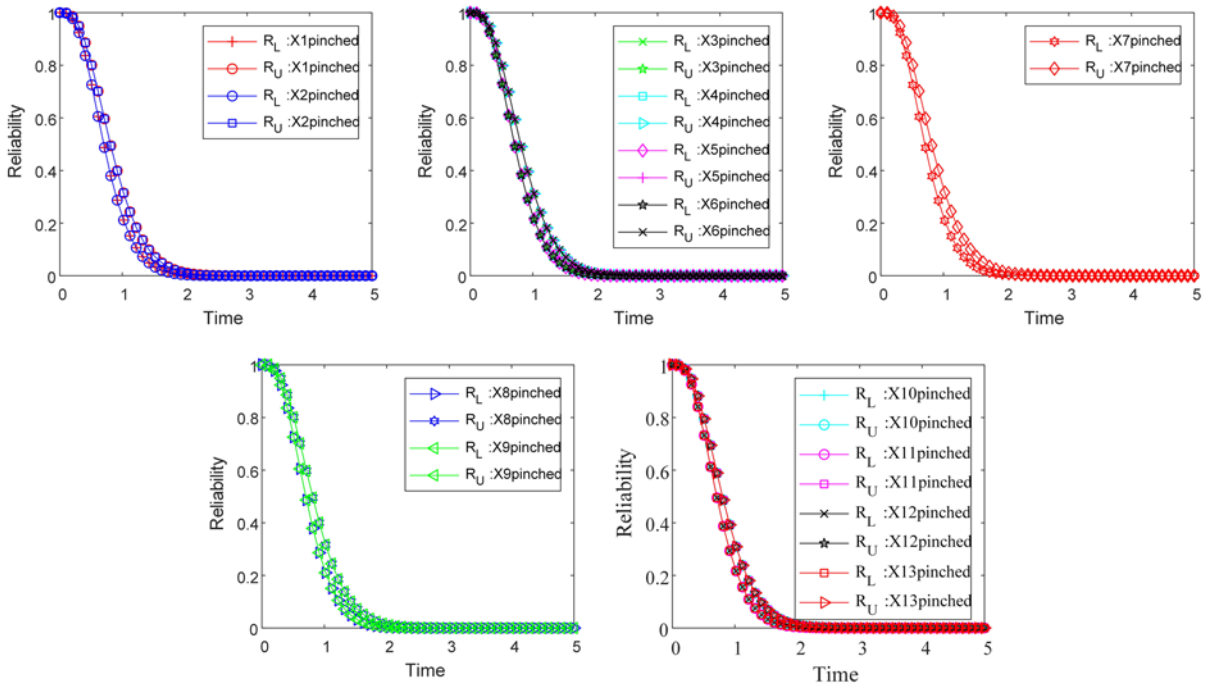

Fig. 7. Reliability p-boxes of components

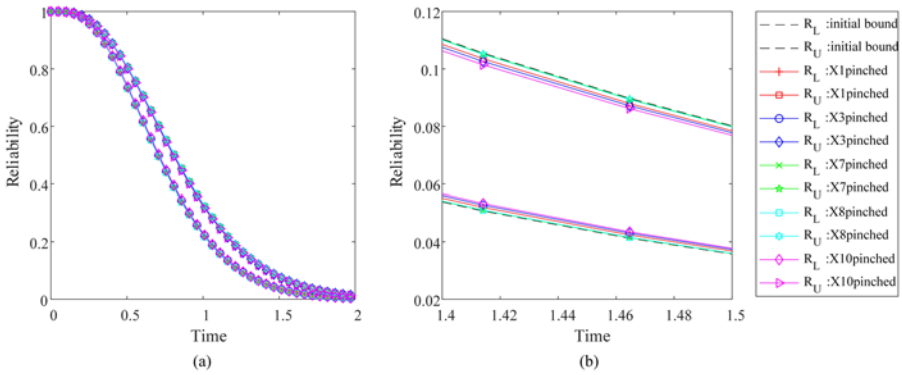

Fig. 8. P-boxes with diverse inputs pinched ((b) is the time interval [1.4, 1.5] of (a))

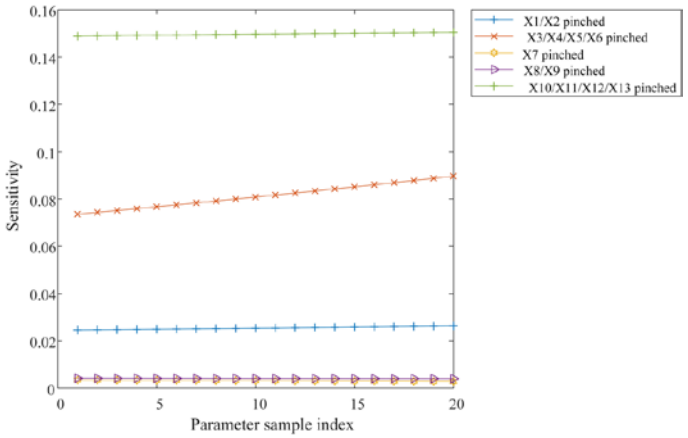

Fig. 9. Deviation of sensitivity

tion of the hydraulic subsystem. Meanwhile, the powertrain system is a key subsystem, which includes a turbine, a reducer and a pump. For the power supply subsystem, two valves are included in the emergency work mode, while only one main valve is contained in the main working mode. Based on the relationships among the components, the fault tree of the system can be plotted as shown in Fig. 12.

To introduce the method and simplify the calculations, the following assumptions are made for system reliability modeling:

1) A component or subsystem has the same failure probability distribution as its corresponding assembly component.

2) Components and subsystems whose failures rarely occur or do not cause system failure are negligible.

Assume that the failure probability of the basic components follows the Weibull distribution and lognormal distribution, respectively, according to the mechanical and electrical characteristics of the system. Additionally, based on accelerated life

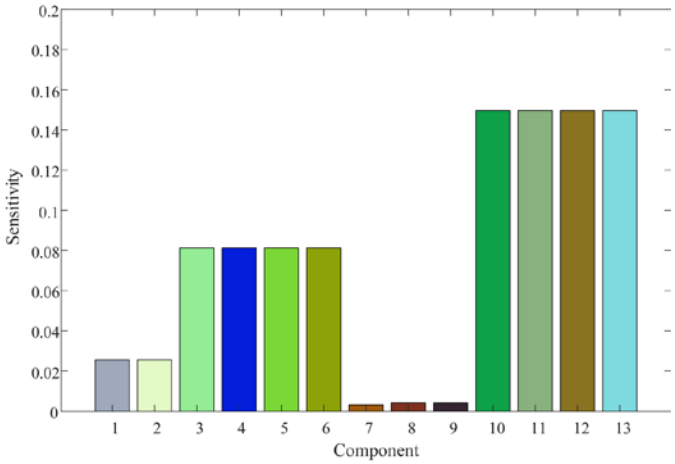

Fig. 10. Mean sensitivity of 13 components

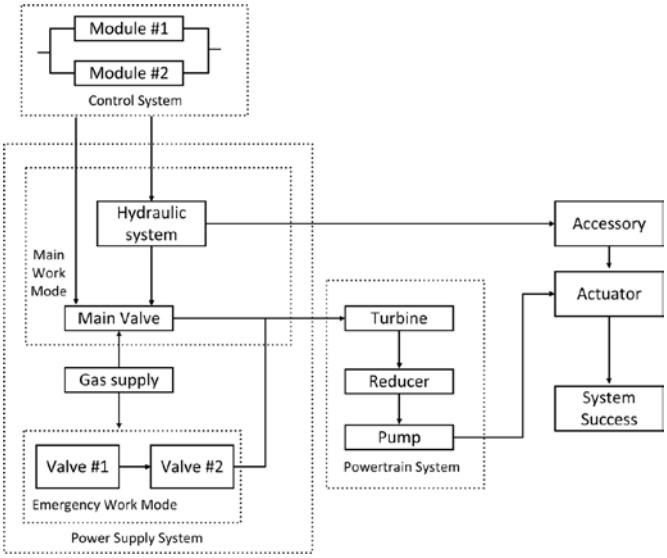

Fig. 11. Functional block diagram of an electromechanical control system

Table 6. Number and description of the events in the system

No.	Event description	No.	Event description
S	Complex electromechanical system task failure	X_3	Turbine failure
Y_1	Control system failure	X_4	Reducer failure
Y_2	Powertrain system failure	X_5	Pump failure
Y_3	Power is not transmitted to the subordinate unit	X_6	Valve #1 failure
Y_4	Main work mode failure	X_7	Valve #2 failure
Y_5	Emergency work mode failure	X_8	Main valve failure
X_1	Control module #1 failure	X_9	Hydraulic system failure
X_2	Control module #2 failure		

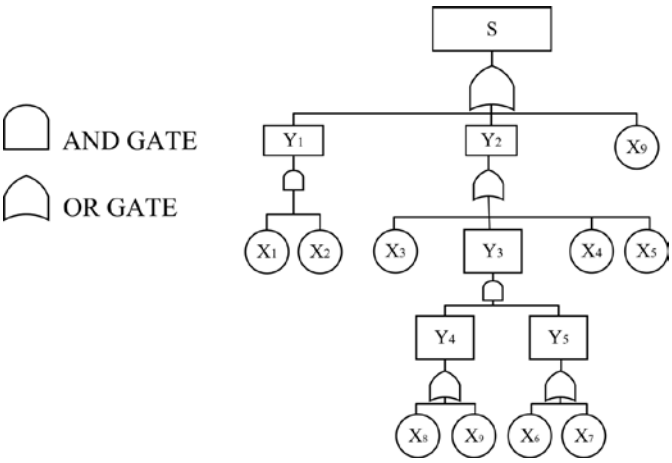

Fig. 12. Fault tree of the electromechanical control system

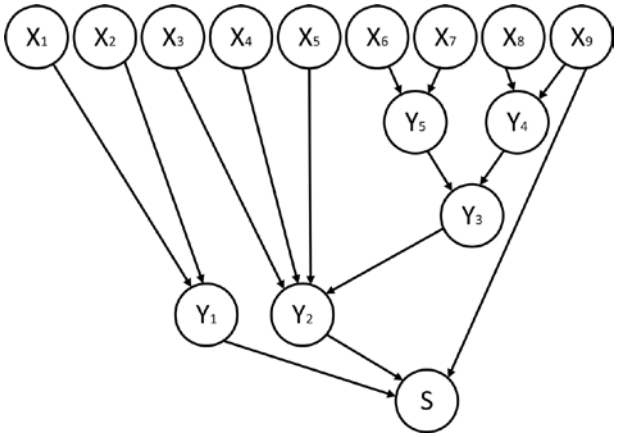

Fig. 13. BN of the electromechanical control system

testing and field data analysis, Table 7 lists the life distribution and life interval of different subsystems and components of the above-mentioned system [10].

4.2. System reliability modeling

Since it is necessary to obtain both the DAG and CPTs for the construction of a BN, the DAG can first be obtained and shown as based on the fault tree in Fig. 12. Meanwhile, owing to the forward reasoning requirement of a BN, it is essential to provide the matrix form of the DAG denoted as D, where the element $d_{i,j}$ in the matrix can be represented by Eq. (15).

$$\begin{cases} d_{1,10} = d_{2,10} = 1 \\ d_{3,11} = d_{4,11} = d_{5,11} = d_{12,11} = 1 \\ d_{6,14} = d_{7,14} = 1 \\ d_{8,13} = d_{9,13} = 1 \\ d_{13,12} = d_{14,12} = 1 \\ d_{10,15} = d_{11,15} = d_{9,15} = 1 \\ \text{else} \ = 0 \end{cases} \tag{15}$$

Additionally, the CPTs can be represented as the form of matrices CPT_{Y_1}, CPT_{Y_2}, CPT_{Y_3}, CPT_{Y_4}, CPT_{Y_5} and CPT_S referred to by the specifications of CPTs corresponding to AND and OR relations

Table 7. Distribution parameters of basic units

No.	Parameters	No.	Parameters
X_1	$\beta_1=\beta_2=2.769$; $\eta_1=\eta_2=[4794.4,5381.5]$	X_6	$\mu_6=[7.2442,7.5700]$; $\sigma_6=0.1980$
X_2		X_7	$\mu_7=[7.2442,7.5700]$; $\sigma_7=0.1980$
X_3	$\beta_3=6.02$; $\eta_3=[7439.4,7752.6]$	X_8	$\mu_8=[8.4287,8.5937]$; $\sigma_8=0.1003$
X_4	$\beta_4=1.935$; $\eta_4=[8459.8,9746.6]$	X_9	$\mu_9=[8.3428,8.4692]$; $\sigma_9=0.0768$
X_5	$\beta_5=8.33$; $\eta_5=[5851.9,5999.3]$		

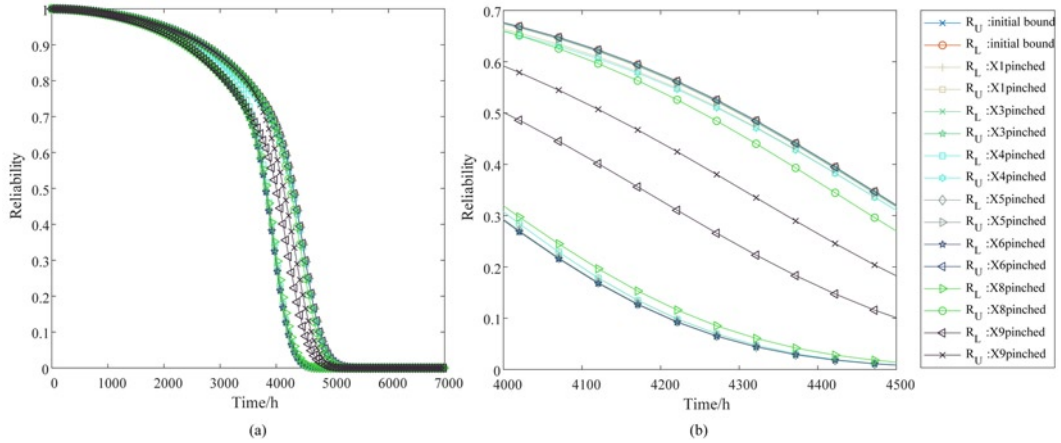

Fig. 14. P-boxes of different types of components with pinched uncertainty and initial bounds ((b) is the time interval (4000, 4500) of (a))

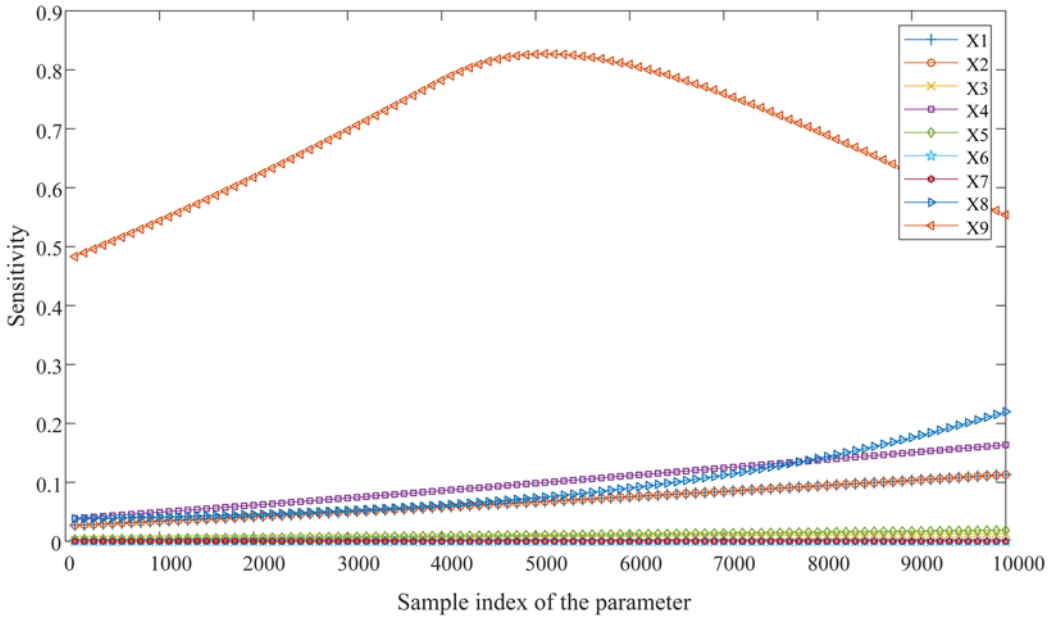

Fig. 15. Sensitivity deviation of each component

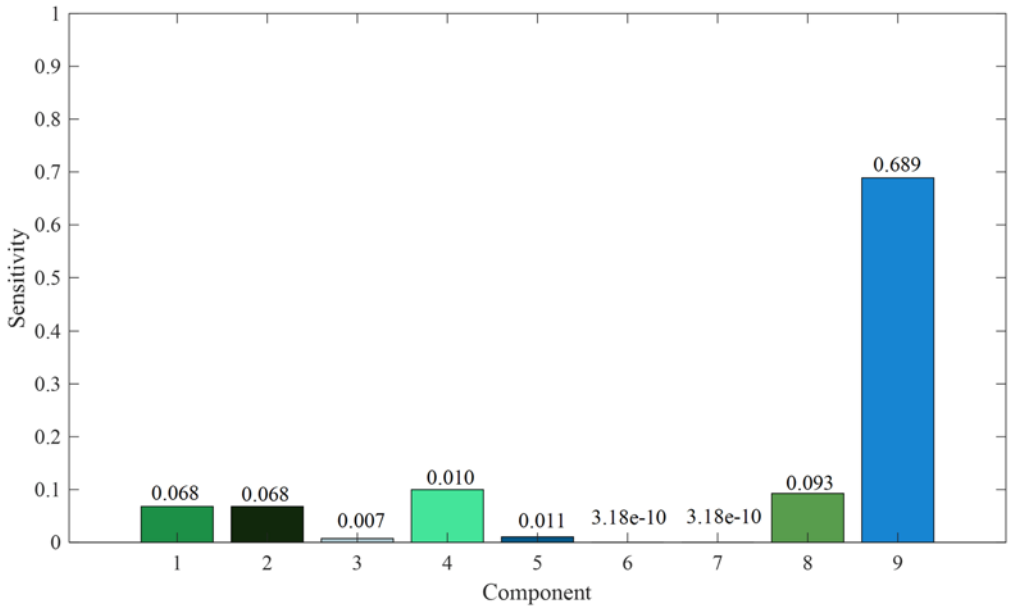

Fig. 16. Mean sensitivity of components X_1~X_9

described in Section 2.1. Particularly, for the system, since X_6-X_7 and X_1-X_2 have the same probability distribution and are in the same connection, they can be regarded as equivalent according to Section 3. $f_{i,j}^k$ and $\overline{f_{i,j}^k}$ in the input vectors F and $F_{i,j}^k$ are obtained by the methods described in Table 7 and Section 3.2.1, where $l_k = 7$, $l_c = 9$ and $l_s = 10000$. The Bayesian forward reasoning and reliability characterization can be performed according to Eq. (11) and Eq. (12). On the other hand, due to the uncertainty in the input vector, the system reliability is uncertain and can be characterized by the p-box described in Section 3.3.

As shown in Fig. 14, there are several curves related to reliability bounds with each component pinched. It is obvious that component X_9 has the most critical impact on p-box uncertainty space compression after reducing the epistemic uncertainty of 9 types of components. However, it is difficult to distinguish the reduction effect of the other 8 components owing to the large number of curves crossing shown in Fig. 14. Hence, it is beneficial to further perform a sensitivity analysis of the system to resolve the aforementioned issues as well as obtain an accurate assessment indicator.

4.3. Sensitivity index and ranking

Based on Eq. (7) and the description of SA mentioned in Section 3.4, the epistemic uncertainty space size of the 10 sets of probability bounds in Fig. 14 should be estimated according to Eq. (6). Moreover, since it is difficult to determine the distribution of the target probability, the sensitivity might be biased. Therefore, to sample the parameter interval to offset the effect of the bias as described in Section 3.4, the sample size is chosen as l_s=10000. As depicted in Fig. 15, the ordinates, which refer to the sensitivity with the input vector of $F_{i,\mathrm{j}}^k$, are denoted as the reduction ratio of the uncertainty space with a maximum value of 1. From the results, it can be noted that the sensitivity changes of subsystem X_9, i.e., the hydraulic system, are nonlinear and much higher than those of X_1~X_8. Hence, the hydraulic system is the subsystem with the greatest uncertainty effect on the electromechanical system, which means that as the uncertainty of the system reliability must be reduced, a comprehensive analysis of the hydraulic system should be considered first. In contrast, the curves of X_3,X_5,X_6,X_7 are almost close to the x-axis with a large distance to X_1,X_2,X_4,X_8,X_9. Thus, it can be noted that X_3,X_5,X_6 and X_7 have the least impact on the system uncertainty, where the evaluation for system uncertainty reduction should be given the lowest consideration or even be deemed negligible. Furthermore, it is difficult to rank the sensitivity of X_1~X_8 since the curves are staggered with each other at similar amplitudes. Therefore, according to Eq. (8) and the method detailed in Section 3.4, we need to calculate the mean of each component sensitivity shown in Fig. 15 and plot the bar graph as shown in Fig. 16. Specifically, as seen in Fig. 16, the sensitivity of X_4, i.e., the reducer, is slightly higher than that of X_1, X_2 and X_8 but much higher than that of X_3, X_5, X_6 and X_7. Additionally, both X_3 and X_5 should be in the lower consideration of the system uncertainty reduction since their impact on the system uncertainty is just slightly higher than that of X_6 and X_7.

5. Conclusion

Sensitivity analysis has prominent application in the risk and reliability analysis field to explore how changes in the inputs of the component affect the outputs of the system. Nevertheless, the current SA study is mostly relevant to random variables with precise probability parameters, thus ignoring the existence of epistemic uncertainty. As industrial requirements increase, ISA theories have become popular solutions due to the inescapable imprecision in engineering. The target of the proposed method is to assess the reliability and sensitivity of mechatronic systems by considering the epistemic uncertainty and simultaneously accomplishing the sensitivity analysis.

In this paper, a pinching method was proposed to identify the sensitive components in a complex system on the basis of the reliability model established by the BN, and epistemic uncertainty is manipulated by the p-box. This method, on the basis of the BN reliability model, provides an alternative sensitivity index, unlike other methods such as Sobol indices [18], to successfully identify the components and subsystems with high sensitivity, which is an efficient way for engineers to reduce epistemic uncertainty. Moreover, compared with traditional Monte Carlo approaches, the brief concept and formulas of the p-box support a more intuitive SA and reduce the computational complexity. Two cases were applied to prove the feasibility, and we induce the sensitivity ranking via Fig. 10 and Fig. 16. Obviously, the accuracy of identifying the sensitive components is satisfactory. Particularly in the case of the electromechanical system from Ref. [10], the results show that the system epistemic uncertainty can be reduced by approximately 80% by pinching the uncertainty of the hydraulic system. Hence, efforts to reduce imprecision should primarily be made in hydraulic systems. During the analyses, this approach opens a new pathway based on the Bayesian network and pinching method in reliability sensitivity assessment, which indicates an efficient direction for mitigating engineering efforts in uncertainty reduction. In addition, during the analysis process, we also encountered several shortcomings. The sensitivity deviation cannot be totally eliminated by calculating the mean value. Therefore, our future work will focus on the selection and comparison of various sensitivity indices to improve the performance of the ISA method.

Acknowledgment

This work was partially supported by the National Natural Science Foundation of China under contract No. 51805073 and U1830207, the Chinese Universities Scientific Fund under contract No. ZYGX2018J061, the China Postdoctoral Science Foundation under contract No. 2015M582536, and the Sichuan Science and Technology Project under contract No. 2019JDJQ0015.

References

1. Guo H, Yang X. A simple reliability block diagram method for safety integrity verification. Reliability Engineering & System Safety 2007; 92(9): 1267-1273, https://doi.org/10.1016/j.ress.2006.08.002.
2. Simon C, Weber P, Evsukoff A. Bayesian networks inference algorithm to implement Dempster Shafer theory in reliability analysis. Reliability Engineering & System Safety 2008; 93(7): 950-963, https://doi.org/10.1016/j.ress.2007.03.012.
3. Simon C, Weber P, Levrat E. Bayesian Networks and Evidence Theory to Model Complex Systems Reliability. JCP 2007; 2(1): 33-43, https://doi.org/10.4304/jcp.2.1.33-43.
4. Ericson C A. Fault tree analysis. System Safety Conference, Orlando, Florida, 1999; 1: 1-9.
5. Pearl J. Fusion, propagation, and structuring in belief networks. Artificial Intelligence 1986; 29(3): 241-288, https://doi.org/10.1016/0004-

3702(86)90072-X.
6. Cai B, Liu Y, Liu Z, Tian X, Dong X, Yu S. Using Bayesian networks in reliability evaluation for subsea blowout preventer control system. Reliability Engineering & System Safety 2012; 108: 32-41, https://doi.org/10.1016/j.ress.2012.07.006.
7. Su C, Fu Y. Reliability assessment for wind turbines considering the influence of wind speed using bayesian network. Eksploatacja i Niezawodnosc -Maintenance and Reliability 2014; 16(1): 1-8.
8. Mi J, Li YF, Beer M, Broggi M, Cheng Y. Importance measure of probabilistic common cause failures under system hybrid uncertainty based on bayesian network. Eksploatacja i Niezawodnosc - Maintenance and Reliability 2020; 22(1): 112-120, https://doi.org/10.17531/ein.2020.1.13.
9. Bi S, Broggi M, Wei P, Beer M. The Bhattacharyya distance: Enriching the p-box in stochastic sensitivity analysis. Mechanical Systems and Signal Processing 2019; 129: 265-281, https://doi.org/10.1016/j.ymssp.2019.04.035.
10. Mi J, Li YF, Yang YJ, Peng W, Huang HZ. Reliability assessment of complex electromechanical systems under epistemic uncertainty. Reliability Engineering & System Safety 2016; 152: 1-15, https://doi.org/10.1016/j.ress.2016.02.003.
11. Xiahou T, Liu Y. Reliability bounds for multi-state systems by fusing multiple sources of imprecise information. IISE Transactions 2019; 0(0): 1-18, https://doi.org/10.1080/24725854.2019.1680910.
12. Dempster A P. The Dempster-Shafer calculus for statisticians. International Journal of approximate reasoning 2008; 48(2): 365-377, https://doi.org/10.1016/j.ijar.2007.03.004.
13. Misuri A, Khakzad N, Reniers G, Cozzani V. Tackling uncertainty in security assessment of critical infrastructures: Dempster-Shafer Theory vs. Credal Sets Theory. Safety Science 2018; 107: 62-76, https://doi.org/10.1016/j.ssci.2018.04.007.
14. Aguirre F, Sallak M, Schön W. Construction of Belief Functions From Statistical Data About Reliability Under Epistemic Uncertainty. IEEE Transactions on Reliability 2013; 62(3): 555-568, https://doi.org/10.1109/TR.2013.2273047.
15. Yang J, Huang HZ, He LP, Wen D, Zhu S-P. Failure Mode and Effects Analysis of Compressor Blades of Aeroengines Using Dempster-Shafer Evidence Theory. American Society of Mechanical Engineers Digital Collection: 2012: 863-870.
16. Mi J, Li YF, Peng W, Huang H-Z. Reliability analysis of complex multi-state system with common cause failure based on evidential networks. Reliability Engineering & System Safety 2018; 174: 71-81, https://doi.org/10.1016/j.ress.2018.02.021.
17. Feng G, Patelli E, Beer M, Coolen F P A. Imprecise system reliability and component importance based on survival signature. Reliability Engineering & System Safety 2016; 150: 116-125, https://doi.org/10.1016/j.ress.2016.01.019.
18. Schöbi R, Sudret B. Global sensitivity analysis in the context of imprecise probabilities (p-boxes) using sparse polynomial chaos expansions. Reliability Engineering & System Safety 2019; 187: 129-141, https://doi.org/10.1016/j.ress.2018.11.021.
19. Ferson S, Kreinovich V, Grinzburg L, S.Myers D. Constructing probability boxes and Dempster-Shafer structures. Sandia National Lab. (SNL-NM), Albuquerque, NM (United States) 2015.
20. Wei P, Lu Z, Song J. Variable importance analysis: A comprehensive review. Reliability Engineering & System Safety 2015; 142: 399-432, https://doi.org/10.1016/j.ress.2015.05.018.
21. Wei P, Lu Z, Ruan W, Song J. Regional sensitivity analysis using revised mean and variance ratio functions. Reliability Engineering & System Safety 2014; 121: 121-135, https://doi.org/10.1016/j.ress.2013.08.001.
22. Alvarez D A. Reduction of uncertainty using sensitivity analysis methods for infinite random sets of indexable type. International journal of approximate reasoning 2009; 50(5): 750-762, https://doi.org/10.1016/j.ijar.2009.02.002.
23. Sankararaman S, Mahadevan S. Separating the contributions of variability and parameter uncertainty in probability distributions. Reliability Engineering & System Safety 2013; 112: 187-199, https://doi.org/10.1016/j.ress.2012.11.024.
24. Krzykacz-Hausmann B. An approximate sensitivity analysis of results from complex computer models in the presence of epistemic and aleatory uncertainties. Reliability Engineering & System Safety 2006; 91(10): 1210-1218, https://doi.org/10.1016/j.ress.2005.11.019.
25. Oberguggenberger M, King J, Schmelzer B. Classical and imprecise probability methods for sensitivity analysis in engineering: A case study. International Journal of Approximate Reasoning 2009; 50(4): 680-693, https://doi.org/10.1016/j.ijar.2008.09.004.
26. Helton J C, Johnson J D, Oberkampf W L, Sallaberry C J. Sensitivity analysis in conjunction with evidence theory representations of epistemic uncertainty. Reliability Engineering & System Safety 2006; 91(10): 1414-1434, https://doi.org/10.1016/j.ress.2005.11.055.
27. Ferson S, Troy Tucker W. Sensitivity analysis using probability bounding. Reliability Engineering & System Safety 2006; 91(10): 1435-1442, https://doi.org/10.1016/j.ress.2005.11.052.
28. Mi J, Cheng Y, Song Y, Bai L, Chen K. Application of dynamic evidential networks in reliability analysis of complex systems with epistemic uncertainty and multiple life distributions. Annals of Operations Research, 2019:1-23, https://doi.org/10.1007/s10479-019-03211-4.
29. Montgomery V. New statistical metliods in risk assessment by probability bounds 2009.
30. Huang X, Coolen F P A. Reliability sensitivity analysis of coherent systems based on survival signature. Proceedings of the Institution of Mechanical Engineers, Part O: Journal of Risk and Reliability 2018; 232(6): 627-634, https://doi.org/10.1177/1748006X18754974.
31. Feng G, George-Williams H, Patelli E, Coolen F P A, Beer M. An efficient reliability analysis on complex non-repairable systems with common-cause failures. Safety and Reliability-Safe Societies in a Changing World-Proceedings of the 28th International European Safety and Reliability Conference; 2018: 2531-2538, https://doi.org/10.1201/9781351174664-318.

He LIANG
School of Automation Engineering,
University of Electronic Science and Technology of China,
No.2006, Xiyuan Ave, West Hi-Tech Zone, Chengdu, Sichuan, 611731, P.R. China

Jinhua MI
School of Automation Engineering,
Center for System Reliability and Safety,
University of Electronic Science and Technology of China,
No.2006, Xiyuan Ave, West Hi-Tech Zone, Chengdu, Sichuan, 611731, P.R. China

Libing BAI
Yuhua CHENG
School of Automation Engineering,
University of Electronic Science and Technology of China,
No.2006, Xiyuan Ave, West Hi-Tech Zone, Chengdu, Sichuan, 611731, P.R. China

Emails: harrisliang@outlook.com, jinhuami@uestc.edu.cn,
libing.bai@uestc.edu.cn, yhcheng@uestc.edu.cn